NANO LETTERS 18.1 (2018): 602-609

DOI: http://doi.org/10.1021/acs.nanolett.7b04804

Optical forces at the nanoscale: size and electrostatic effects

*Paloma Rodríguez-Sevilla[§,] *, Katarzyna Prorok[||], Artur Bednarkiewicz [∫],Manuel I. Marqués,[β] Antonio García-Martín,[†] José García Solé[§], Patricia Haro-González[§] and Daniel Jaque[§,┼,] **

§ Fluorescence Imaging Group, Departamento de Física de Materiales, Universidad Autónoma de Madrid, 28049 Madrid, Spain.

| Wroclaw Research Centre EIT+, ul. Stabłowicka 147, 54-066 Wrocław, Poland.

∫ Institute of Low Temperature and Structure Research, Polish Academy of Sciences, ul.Okolna 2, 50-422 Wroclaw, Poland.

β Departamento de Física de Materiales, IFIMAC and "Instituto Nicolás Cabrera", Universidad Autónoma de Madrid, 28049 Madrid, Spain.

† IMN- Instituto de Micro y Nanotecnología (CNM-CSIC), Isaac Newton 8, E-28760 Madrid, Spain

┼ Instituto Ramón y Cajal de Investigaciones Sanitarias, Hospital Ramón y Cajal, Madrid 28034, Spain.

KEYWORDS: Nanoparticles, optical trapping, size, zeta potential.

ABSTRACT

The reduced magnitude of the optical trapping forces exerted over sub-200 nm dielectric nanoparticles complicates their optical manipulation, hindering the development of techniques and studies based on it. Improvement of trapping capabilities for such tiny objects requires a deep understanding of the mechanisms beneath them. Traditionally, the optical forces acting on dielectric nanoparticles have been only correlated with their volume, and the size has been traditionally identified as a key parameter. However, the most recently published research results have shown that the electrostatic characteristics of sub-100 nm dielectric particle could also play a significant role. Indeed, at present, it is not clear what do optical forces depend on. In this work we designed a set of experiments in order to elucidate the different mechanism and properties (i.e. size and/or electrostatic properties) that governs the magnitude of optical forces. The comparison between experimental data and numerical simulations have shown that the double layer induced at nanoparticle´s surface, not considered in the classical description of nanoparticle´s polarizability, plays a relevant role determining the magnitude of the optical forces. The here presented results constitute the first step towards the development of dielectric nanoparticle over which enhanced optical forces could be exerted, enabling their optical manipulation for multiples purposes ranging from fundamental to applied studies.

Introduction

Since the 70's, when Arthur Ashkin and coworkers demonstrated that optical forces (OFs) could displace and levitate microsized particles, optical trapping (OT) has been evidenced as one of the most important manipulating tools with real potential applications in numerous areas ranging from biology to physics.[1] Basically, OT is based on the use of a tightly focused laser beam to generate a three-dimensional (3D) optical potential well (optical trap), which dimensions are given by the laser spot size (typically close to 1μm). When a micro or nanoparticle drops into this potential well, its motion is confined within it, provided that the depth of the potential well is larger than the thermal energy of the particle. In these conditions, 3D control over the trapped micro or nanoparticle can be achieved by simple manipulation of the position of the focused laser beam.

During the very last years, OT of nanosized objects have attracted more and more interest from both fundamental and applied points of view.[2-5] Among the nanoparticles (NPs) whose 3D optical manipulation has been demonstrated, dielectric luminescent NPs (LNPs) resulted to be of special importance.[6] This is due to the fact that LNPs could be sensible to the physical conditions of surrounding environment (temperature, chemicals, pH, etc) and, in some cases, they can also be used, for example, to convert light to heat in a controllable and predictable manner.[7-12] Based on these properties, OT of a single LNP has been proposed for 3D contactless bio-sensing and therapy procedures. Despite being already demonstrated, OT of dielectric LNPs is a challenging task since OFs exerted over such small non-absorbing particles are in the range of femtonewtons, which leads to OT potential depths as low as 10^{-21} J, which is of the same order of magnitude as thermal energy at room temperature.[4, 13] Thus, thermal fluctuations act as a relevant destabilizing agent of the optical trap leading to instable OT.[13] Therefore, a route for increasing the trapping efficiency of LNPs is compulsory for the development of reliable remote scanning techniques. As a first step, it

is necessary to reach a full understanding of which physical parameters do exactly determine the magnitude of OFs acting on LNPs. This would allow rational modification of the LNPs for enhancing the OF exerted over them.

Traditionally, the OF has been decomposed into two components.[14, 15] The scattering force (F_{scat}) is associated with the transfer of linear momentum from the scattered photons to the particle. It pushes the particle in the propagation direction of the trapping beam. The confinement of the particle within the optical trap is due to a second force which attracts it towards the highest laser beam intensity region. This is the gradient force (F_{grad}) and, in the range of particles much smaller than the trapping wavelength (Radius << λ), it can be described as the force experienced by an electric dipole in an inhomogeneous electromagnetic field. When dealing with weakly absorbing dielectric nanoparticles (as it is the case of the LNPs studied in this work), these components can be written as:[16]

$$\vec{F}_{grad} = \alpha' \varepsilon_0 \frac{n_m^2}{4} \vec{\nabla}(E^2) \qquad \textbf{(1)}$$

$$\vec{F}_{scat} = k\alpha'' \left\{ \frac{n_m}{c} < \vec{S} > \right\} + k\alpha'' \left\{ \frac{c}{n_m} \vec{\nabla} \times < \overrightarrow{L_S} > \right\} \qquad \textbf{(2)}$$

where $E^2 = EE^*$being E the electric field of the trapping wave, $\varepsilon_0$is the vacuum dielectric constant, $\langle S \rangle$ is the time averaged Poynting vector, $\langle \overrightarrow{L_s} \rangle$ the time averaged spin angular momentum of the electromagnetic field, n_m is the index of refraction of the surrounding medium, c is the speed of light, and $k = 2\pi n_m/\lambda_0$, with λ_0 the trapping wavelength in vacuum. **Equations 1-2** indicate that both F_{grad} and F_{scat} components depend on the electronic polarizability ($\alpha_{NP} = \alpha' + i\alpha''$) of the trapped particle. In previous reference works dealing with optical trapping

of dielectric nanoparticles authors traditionally used the Claussius-Mossotti expression to describe particle´s polarizability. Although the use of this formalism to adequately describe the nanoparticle´s polarizability is limited it has been widely used in the past to describe the physics underlying optical trapping of dielectric nanoparticles and, for instance, to elucidate the size-dependence of optical forces. In a first order approximation, assuming a delta-like (sharp, well defined) nanoparticle-medium interface (see **Figure 1a**), the electronic polarizability given by Claussius-Mossotti formalism can be written as:

$$\alpha = \alpha_0 = 3V_{NP}\frac{\varepsilon_{NP} - \varepsilon_m}{\varepsilon_{NP} + 2\varepsilon_m} \qquad \textbf{(3)}$$

with $\varepsilon_{NP} = {n_{NP}}^2$, and ε_m the relative permittivity of the particle (n_{NP} its refractive index), and that of the surrounding medium, respectively. As can be seen, the total OF (F_{OT}) scales with the particle volume:

$$F_{OT} \sim |\alpha_{NP}| \sim V_{NP} \qquad \textbf{(4)}$$

Under this first order approximation (i.e. pure nanoparticle-medium interface, see **Figure 1a**) the volume of the NP is the only parameter determining the magnitude of OFs. However, recently published works have evidenced that OFs could also depend on the electrostatic properties of the interface between the NP and the surrounding medium. Indeed, it was experimentally demonstrated that the magnitude of OFs can appropriately be enhanced through a controlled modification of the particle-medium interface.[17] These results can be understood in terms of a more complex model in which the NP-medium interface is not supposed to be a delta-like one. Instead, it is assumed that the NP is surrounded by a coating layer that constitutes an effective NP-medium

interface (see **Figure 1b**). This coating could be constituted by either coating molecules or by the charge distribution that moves together with the nanoparticle. Independently of the nature of the NP-medium interface, the polarizability of the NP can be written as:[18]

$$\alpha_{NP} = 3(V_{NP} + V_c)\frac{(\varepsilon_c - \varepsilon_m)(\varepsilon_{NP} + 2\varepsilon_c) + f(\varepsilon_{NP} - \varepsilon_c)(\varepsilon_m + 2\varepsilon_c)}{(\varepsilon_c + 2\varepsilon_m)(\varepsilon_{NP} + 2\varepsilon_c) + f(2\varepsilon_c - 2\varepsilon_m)(\varepsilon_{NP} - \varepsilon_c)} \quad \textbf{(5)}$$

where ε_c is the relative permittivity of the NP-medium interface, V_C the coating volume and $f=V_{NP}/(V_{NP}+V_c)$. In general, all particles present surface charge, even ligand-free (i.e. bare) ones. This leads to the appearance of a "charge cloud" that behaves as a coating layer with a particular relative ε_c. Thus, the electronic polarizability depends not only on the NP volume, but also on its electrostatic characteristics (i.e. on the electrostatic properties of the "charge cloud").

Based on the above discussion, it is expected that both, NP volume and electrostatic characteristics, play a role on the magnitude of OFs acting on LNPs. The relative importance of both characteristics in determining the OFs acting on dielectric nanoparticles is not known, being this an open fundamental question. To answer it, we have designed dielectric upconverting NP (UCNPs), capable to generate visible emission under infrared optical excitation, of intentionally variable size (monitored through transmission electron microscopy (TEM) images) and different charge properties (monitored through the zeta potential). OFs exerted over such UCNPs, which sizes are much smaller than the wavelength of the trapping radiation, have been measured by using the hydrodynamic drag method. Systematic analysis of the trapping strength as a function of particle volume and charge has been carried out to unequivocally determine the role played by both parameters in the range of sizes under study.

Materials and Methods

Optical trapping setup and optical trap characterization. The optical trapping setup is schematically represented in the upper part of **Figure 2a**. The 980 nm trapping radiation generated by a fiber-coupled laser diode was tightly focused, by using a high numerical aperture microscope lens (100x, 1.4NA), into a microchannel (Ibidi Inc., μ-Slide I 80106) where the diluted suspension of UCNPs was placed. When optically trapped (see **Figure 2a**, lower part), the UCNPs emit visible light through an upconversion process after the absorption of the infrared radiation.[19-22] This generated luminescence, which is collected by the same trapping objective, is used for optical visualization of the trapped particles by means of a CCD camera (QImaging). It is important to mention that the size of the studied UCNPs is below the diffraction limit of the lens, thus their luminescence is indispensable for particle detection. The total luminescence intensity at the optical trap position allows the determination of the number of trapped UCNPs. The recorded luminescence as a function of time acquired during a representative experiment is represented in **Figure 2b**. Each time an UCNP is optically trapped, a step-like rise in the total luminescence takes place. By changing the concentration of the colloidal suspension of UCNPs and the trapping power, the number of particles entering the trap for a period of time can be controlled.[4] The luminescence has been monitored in real-time to ensure just a single UCNP was inside the optical trap during OF-determination experiments.

The trapping strength or quality of the optical trap, characterized by the Q-factor (Q), has been measured for a total number of fifteen different UCNPs. The maximum optical force (F_{OT}^{max}) is proportional to the fraction (given by the Q-factor) of the total momentum ($\frac{n_m P_l}{c}$) transferred to the particle:

$$F_{OT}^{max} = Q \frac{n_m P_l}{c} \qquad \textbf{(6)}$$

where P_l is the laser power, n_m the refractive index of the surrounding medium, and c the speed of light. The method used for the characterization of the optical trap was the wide-known hydrodynamic drag method.[15, 23] This approach allows to calibrate the trapping force against a known force which is the hydrodynamic drag force (F_d) that opposes the displacement of a moving object in a fluid:

$$F_d = \frac{6\pi\eta R v}{C} \qquad \textbf{(7)}$$

where C represents the parameter that takes into account the Faxen's correction.[23] **Equation 7** gives the drag force for the specific case of a sphere of hydrodynamic radius R moving inside a fluid of viscosity η. In this equation, v is the relative velocity between the particle and the fluid. This force will drag the particle away from its equilibrium position inside the optical trap if a relative velocity between the particle and the fluid is induced. The particle is trapped (located inside the trap) if $r \leq w_o$, with w_o being the optical trap radius. Likewise, the particle is released from the trap when $r > w_o$. For moderate relative velocities, the particle remains trapped so that it is optically excited by the trapping radiation and, therefore, its visible luminescence is still excited. This situation is schematically represented in **Figure 2c**. In this example, for relative velocities lower than 200 μm/s, the particle remains trapped and the intensity of visible luminescence has a non-zero value. However, when the relative velocity is increased, the particle escapes from the trap because $F_d > F_{OT}^{max}$. When this occurs, the luminescence intensity vanishes evidencing that the particle has been release from the trap. Therefore, the maximum relative velocity at which the particle could move before being released from the trap is given by:

$$F_{OT}^{max} = 6\pi\eta R v_{max} = Q\frac{n_m P_l}{c} \qquad \textbf{(8)}$$

According to **Equation 8,** Q could be measured through the determination of v_{max}. The experimental procedure to determine v_{max} is as follows. Once the particle is optically trapped (luminescence is detected at the trap position), a relative velocity between the particle and the fluid (water) is generated by displacing the microchannel at a certain controlled velocity (by using a motorized stage, see **Figure 2a**) while the optical trap position remains constant. The microchannel is displaced at increasing velocities till a certain velocity is reached ($v > v_{max}$) at which the particle is released. This process is repeated several times for different particles in order to get a reproducible value for v_{max}. Then, by using **Equation 8**, Q is determined by substituting R by the hydrodynamic radius of the particles. The characterization of the optical trap by the drag method instead by using other approaches, such as power spectral density (PSD) measurements, is justified in detail in the Supporting Information. Briefly, we found this method to be straightforward and easier to implement as the determination of v_{max} can be done by recording particle luminescence without requiring single particle detection and tracking. In addition, we found that the experimental uncertainty on the determination of the Q-factor achieved by the drag method is significantly lower than those obtained by using alternative ones. Experiments carried out in our lab and previous works dealing with OF measurements in dielectric sub-100 nm nanoparticles have concluded that experimental uncertainties can be significantly reduced when measuring the Q-factor by the drag method instead of by using PSD-based measurements (see **Table S1** in Supporting Information).

Dielectric upconverting nanoparticles. Two different particle geometries were studied: disc-like and spherical. Representative TEM images of the two types of studied particles can be found in **Figure 3**. Eight different sized disc-like UCNPs (**Figure 3a**) and seven core-shell spherical UCNPs with increasing diameter (**Figure 3b**) and different zeta potential were studied. Core-shell spherical particles are composed of an upconverting core coated by a silica shell. The upconverting

core is made of sodium yttrium fluoride ($NaYF_4$) doped with Er^{3+} and Yb^{3+} ions. The shell thickness of all the samples differs, while the core remains the same. Core-shell particles are represented by grey and green dots. Disc-like particles are also made of $NaYF_4$ doped with Er^{3+} and Yb^{3+} ions. After the synthesis process, the ligands at the surface of these particles were removed to obtain bare NPs. For more information regarding particle synthesis and characterization see Supporting Information. It could be noted that disc-like particles have a spheroidal shape for sizes shorter than 30 nm. Hexagonal facets as those shown in **Figure 3a** are only seen for particle's radius larger than 30 nm. Despite this fact, all these particles are going to be referred as disc-like UCNPs and represented by hexagonal light green dots. Both kinds of particles are codoped with Er^{3+} and Yb^{3+} ions since this particular combination of dopants leads to an intense visible luminescence (adequate for the presented detection system) under 980 nm optical excitation (the used trapping wavelength).

For the purpose of this study, the zeta potential of each particle size has been measured. These results are included in **Figure 4**. For the disk-like particles the zeta potential was that of as-synthetized nanoparticles, i.e. no post-synthesis procedure was performed to modify their zeta potential. As can be seen, zeta potential values for the disc-like particles (**Figure 4a**) range from 27 to 47 mV. The zeta potential of the different core-shell UCNPs used in this work is shown in **Figure 4b**. In this case, the zeta potential of four of those samples was that obtained after synthesis procedure, without performing any modification procedure. However, the zeta potential of the largest core-shell particles was varied by adding acetic acid to the solution (see the Supporting Information) in order to obtain core-shell particles with a reduced zeta potential value (in absolute values). It is worth mentioning that, as described in the Supporting Information, the amount of acetic acid added to the aqueous solution is below 0.5 wt %, so that the change induced in the

water viscosity is negligible (thus, it has not need to be taken into account in the Q-factor measurements here performed by the drag method).[24] TEM radius for both geometries are in the range of 5 to 100 nm. It is important to mention that this size range is well below the optical trapping wavelength (980nm) and the trap radius (0.4 μm).

Results and discussion

Figure 5a shows the measured Q values as a function of the UCNP volume for all the studied samples, and those published in [17] (simple dark green dots) for 8 nm in diameter UCNPs which electrostatic characteristics were intentionally modified. The measured values are similar to those already reported for this kind of particles.[17, 25, 26]. Independently of the net value obtained for Q, what is of high relevance in the data included in **Figure 5a** is that no clear linear relation between Q and particle volume is found. This is especially evident for the spherical particles (grey and green dots) and the smallest hexagonal particles (light green hexagons). In addition, data included from [17] shows different Q values for same sized particles, a behaviour that was not explained before. Indeed, experimental data included in **Figure 5a** suggests that for particle volumes well below 80 x10^5 nm^3 (effective radius much smaller than 120 nm) OFs are size independent. Note that for the particular case of the core-shell particles here studied, Q remains practically constant despite the volume is increased by one order of magnitude. The fact that OFs do not scale linearly with the particle volume clearly indicates that the model assuming a delta-like nanoparticle-medium interface (**Figure 1a**) seems to be inadequate since it predicts a linear relation between Q and particle volume.

At this point we would like to note that the size independent values of OFs for sub-100 nm UCNPs cannot be considered as a singularity of these particular particles. L. Jauffred and L.B.

Oddershede performed a systematic study on the OF exerted on single colloidal semiconductor quantum dots (QDs) with different radius ranging from 5 up to 15 nm under experimental conditions very similar to those used in this work.[27] What they concluded is that in this size range the magnitude of OFs and the trap stiffness was size independent. Thus, all the experimental studies performed up to now (including this work) points out that, for sub-100 nm non-metallic nanoparticles (dielectric or semiconductor NPs), size is not the dominant parameter determining the OFs exerted on them, although it could play a secondary role. We would like to note that the size-independent behaviour disagrees, not only with the predictions made based on the Claussius-Mossotti formalism (whose applicability to our nanoparticles might be questioned) but also with rigorous numerical calculations based on the Maxwell Stress Tensor, where the scattered fields have been obtained, with no approximations, using the FDTD framework. **Figure 6a** includes the numerically calculated normalized OFs as a function of particle to trap distance as obtained for six representative particles. **Figure 6b** shows the size-dependence of the Q-factor for the two families of UCNPs used in this work as obtained from data included in **Figure 6a**. Details about the calculation procedures can be found in the Supporting Information. Note that the numerical calculations, predict a linear relation between the OFs and the volume for the two type of particles studies in this work. Discrepancy between numerical simulations and experimental data reveals that other factors different from size, shape, and refractive index contrast (all of them considered in the present numerical simulations) have a mayor impact in the determination of the OFs acting over sub-100 nm dielectric nanoparticles. It is also worth mentioning that the experimentally found non-direct relation between OFs and particle´s volume can be attributed to a finite penetration of the electromagnetic field inside the nanoparticle. To discard this possibility, numerical simulations of the distribution of the electromagnetic field along the particle volume were also conducted (see

Supporting Information). The numerical results show a completely penetration of the electromagnetic field into the volume of the particle, as expected for non-absorbing dielectric particles.

Once the particle size has been dismissed as dominant factor determining OFs on UCNPs, the model assuming a delta-like particle-medium interface (**Figure 1a**) shall be disregarded as well. Thus, experimental results have to be described in terms of the model schematically represented in **Figure 1b**. This implies that, not only the NP and the medium, but also the charge shell between them must be considered. In our case (bare NPs), this intermediate shell is constituted by the "charge cloud" that is induced in the surroundings of the NPs. This "charge cloud" has a double layer structure that can be described, in a first order approximation, by the so-called Electric Double Layer (EDL) approximation.[28] The rigid inner shell is formed by charges tightly attached to the particle with opposite sign to that of the particle surface. The outer layer is composed of charges attracted to the surface charge via the Coulomb interaction. This second layer, also called "diffuse layer", is constituted by free ions and charges that move together with the NP as a result of the balance between coulomb forces and diffusion. The plane defining the extension of the diffuse layer is named the Slipping plane. Characterization of the EDL of NPs is not an easy task. It is widely assumed that the only reliable path for the characterization of the EDL is the so-called zeta potential (ζ) defined as the potential difference between the Slipping plane and a point in the bulk fluid (with net charge zero) away from the NP. Zeta potential of a NP is, indeed, an indicative of its net charge ($|\sigma|$), as the latter is given by:[29]

$$|\sigma| = \frac{2\varepsilon_s\varepsilon_0\kappa k_B T}{e}\left|sinh\left(\frac{e\zeta}{2E_r}\right)\right| \qquad \textbf{(9)}$$

where e is the electron´s charge, κ is the characteristic Debye length, and $sinh$ is the hyperbolic sine function. E_r is a reference energy that represents the minimum electrostatic energy that leads to the stable formation of the EDL. In a first order approximation this can be assumed to be equal to the thermal energy (i.e. $E_r = k_B T$) that is close to 25 meV at room temperature. Thus, **Equation 9** clearly reveals that the electrostatic characteristics of the EDL can be well parametrized by the value of the zeta potential. **Figure 5b** shows the experimentally determined Q values as a function of the zeta potential for each studied UCNPs. The values previously published (dark green dots) for UCNPs, which zeta potential was increased by a chemical protocol (see Supporting Information), are also included.[17] In contraposition to the results from the size effect analysis (**Figure 5a**), a clear trend is now observed which is fulfilled by most of the samples. In general, the magnitude of OFs increases with the absolute value of the zeta potential, and remains constant for values of $|\zeta|$ below c.a. 25 mV. At this point we hypothesise that for UCNPs with sizes below 200 nm, the net polarizability is mainly governed by the electronic polarizability of the EDL (α_{EDL}), so that we can write: $\alpha_{NP} \approx \alpha_{EDL}$. The exact value of α_{EDL} is not known and, to our knowledge, there are no published works which establish it. Our results suggest that the electronic polarizability of the "charge cloud" surrounding the NP is affected by its net charge. Although the exact relation between the electronic polarizability of the EDL and its charge is unknown, here we have assumed that α_{EDL} is proportional to the net charge of the EDL (i.e. to $|\sigma|$). Thus, under this rough approach, we would have:

$$Q \propto \alpha_{NP} \approx \alpha_{EDL} \propto |\sigma| \propto \left|sinh\left(\frac{e\zeta}{2E_r}\right)\right| \qquad \textbf{(10)}$$

Therefore, Q should scale with $\left|sinh\left(\frac{e\zeta}{2E_r}\right)\right|$. The red line in **Figure 5b** shows the best fit of experimental Q vs ζ to **Equation 10**. A reasonable agreement is found since $sinh$ function

reproduces the experimentally observed behaviour, i.e. it foresees an almost constant OF for small values of ζ, whereas it predicts a superlinear growth for ζ values above 30 mV. The best fit is obtained for $E_r = 5$ meV. This is different but comparable to the value predicted by theory ($E_r = k_B T = 25\ e\ mV$). In our opinion, the results included in **Figure 5b** indicate that, for dielectric NPs with sizes below 100 nm, OFs acting on them are mainly governed by the electrostatic properties of the EDL surrounding them.

At this point a fundamental question arises: Is it possible to ascribe to a single particle the zeta potential value obtained for "bulk" measurements, i.e. performed on a colloidal solution containing a non-perfectly homogeneous population of NPs? In this sense we have to point out that, as it has been already published, the zeta potential values estimated from conventional bulk zeta potential measurements and those obtained from direct single particle measurements are equivalent.[30] In addition, for each particle and experimental condition, optical forces were systematically measured over different nanoparticles to perform statistical analysis. The uncertainty of OF measurements were calculated in each case and included as error bas in **Figure 5**. Note that uncertainties are smaller than the net effect observed, particularly in the Q vs zeta potential graph. Therefore, based on previous works and the reduced experimental uncertainties we state that the use of the average zeta potential can be used to describe the zeta potential of the individual particles in the colloidal solution.

Conclusions

Optical forces acting on a great variety of sub-wavelength dielectric nanoparticles (4 – 100 nm in radius) have been measured by using the hydrodynamic drag method. Results have been analysed considering their size and electrostatic properties. No direct correlation between

particle's size (volume) and the magnitude of optical forces has been evidenced. These results are in good agreement with those previously published for semiconductor nanocrystals, revealing that in this size regime (particles with a size much smaller than the wavelength of trapping radiation) size cannot be considered as the only parameter determining the magnitude of the optical forces. Experimental data has revealed that, indeed, optical forces acting on sub-100 nm dielectric nanoparticles are strongly correlated with the zeta potential of the trapped particles. It has been found that, for nanoparticles exhibiting absolute zeta potential value below 25 mV, the exerted optical force is weak whereas for higher zeta potential values ($\zeta > 25\, mV$) optical forces have been found to increase significantly. Conventional dipolar or full numerical solvers for the Maxwell equations have been proven to be unable to explain the experimental findings as they predict, for a given material and medium, size as the governing parameter determining the magnitude of optical forces. The experimental data and their discrepancy with numerical simulations have been explained by a phenomenological model in which the magnitude of optical forces is assumed to be mainly given by the electrostatic charge of the nanoparticle which is quantified by its zeta potential, following a hyperbolic sine function.

The results here obtained constitute the first step towards the optimized design of dielectric sub-wavelength nanoparticles which electrostatic characteristics make them suitable to be trapped with enhanced optical forces. This shall boost the development of optical dielectric probes for multiple applications.

ASSOCIATED CONTENT

Supporting Information.

Synthesis procedures, modification, and characterization of the samples. Experimental issues. Theoretical calculations. The Supporting Information is available free of charge.

AUTHOR INFORMATION

Corresponding Authors

* E-mail: daniel.jaque@uam.es.

* E-mail: paloma.rodriguez@uam.es

Author Contributions

The manuscript was written through contributions of all authors. All authors have given approval to the final version of the manuscript.

Funding Sources

This work has been supported by the Spanish Ministerio de Economia y Competitividad (project Nr.MAT2016-75362-C3-1-R), FIS2015-69295-C3-3-P and the "María de Maeztu" Program Ref: MDM-2014-0377.

ACKNOWLEDGMENT

P.R.S. thanks MINECO and the Fondo Social Europeo (FSE) for the "Promoción del talento y su Empleabilidad en I+D+i" statal program (BES-2014-069410). K.P. acknowledges financial support from the National Science Center Poland (NCN) under the ETIUDA doctoral scholarship on the basis of decision number DEC-2014/12/T/ST5/00646. A.B. acknowledges the statutory financial support from ILT&SR PAS. P.H.G. thanks MINECO for the Juan de la Cierva program (IJCI-2015- 24551). The European Upconversion Network (COST Action CM1403) is

acknowledged. Authors acknowledge R.G. Geitenbeek and J. Fokkema for providing them with the core-shell nanoparticles.

ABBREVIATIONS

LNPs, luminescent nanoparticles; NPs, nanoparticles; OFs, optical forces; optical trapping (OT); TEM, transmission electron microscopy; 3D, three-dimensional; UCNPs, upconverting NP.

REFERENCES

1. Ashkin, A.; Dziedzic, J. M. *Science* **1975,** 187, 1073-1075.
2. Aigouy, L.; Tessier, G.; Mortier, M.; Charlot, B. *Appl. Phys. Lett.* **2005,** 87, 184105.
3. Arita, Y.; Ploschner, M.; Antkowiak, M.; Gunn-Moore, F.; Dholakia, K. *Opt. Lett.* **2013,** 38, 3402-3405.
4. Rodríguez-Sevilla, P.; Rodríguez-Rodríguez, H.; Pedroni, M.; Speghini, A.; Bettinelli, M.; Solé, J. G.; Jaque, D.; Haro-González, P. *Nano Lett.* **2015,** 15, 5068-5074.
5. Gordon, R.; Blakely, J. T.; Sinton, D. *Phys. Rev. A* **2007,** 75, 055801.
6. Baral, S.; Johnson, S. C.; Alaulamie, A. A.; Richardson, H. H. *Applied Physics A* **2016,** 122, 1-8.
7. Christ, S.; Schaferling, M. *Methods and Applications in Fluorescence* **2015,** 3.
8. Lei, P. P.; Liu, X. L.; Dong, L. L.; Wang, Z.; Song, S. Y.; Xu, X.; Su, Y.; Feng, J.; Zhang, H. J. *Dalton Trans.* **2016,** 45, 2686-2693.
9. Ai, X.; Ho, C. J. H.; Aw, J.; Attia, A. B. E.; Mu, J.; Wang, Y.; Wang, X.; Wang, Y.; Liu, X.; Chen, H.; Gao, M.; Chen, X.; Yeow, E. K. L.; Liu, G.; Olivo, M.; Xing, B. *Nat. Commun.* **2016,** 7, 10432.
10. Chen, G.; Qiu, H.; Prasad, P. N.; Chen, X. *Chemical Reviews* **2014,** 114, 5161-5214.
11. Marciniak, L.; Pilch, A.; Arabasz, S.; Jin, D.; Bednarkiewicz, A. *Nanoscale* **2017,** 9, 8288-8297.
12. Bednarkiewicz, A.; Wawrzynczyk, D.; Nyk, M.; Strek, W. *Applied Physics B* **2011,** 103, 847-852.
13. Ashkin, A.; Dziedzic, J. M.; Bjorkholm, J. E.; Chu, S. *Opt. Lett.* **1986,** 11, 288-290.
14. Ashkin, A. *Proceedings of the National Academy of Sciences* **1997,** 94, 4853-4860.
15. Neuman, K. C.; Block, S. M. *Rev. Sci. Instrum.* **2004,** 75, 2787-2809.
16. Albaladejo, S.; Marqués, M. I.; Laroche, M.; Sáenz, J. J. Phys. Rev. Lett. **2009,** 102, 113602-113606.
17. Rodríguez-Rodríguez, H.; Rodríguez Sevilla, P.; Martín Rodríguez, E.; Ortgies, D. H.; Pedroni, M.; Speghini, A.; Bettinelli, M.; Jaque, D.; Haro-González, P. *Small* **2015,** 11, 1555-1561.
18. Bohren, C. F.; Huffman, D. R., Particles Small Compared with the Wavelength. In *Absorption and Scattering of Light by Small Particles*, Wiley-VCH Verlag GmbH: 2007; pp 130-157.
19. Ding, M.; Yin, S.; Chen, D.; Zhong, J.; Ni, Y.; Lu, C.; Xu, Z.; Ji, Z. *Appl. Surf. Sci.* **2015,** 333, 23-33.

20. Dong, B.; Hua, R. N.; Cao, B. S.; Li, Z. P.; He, Y. Y.; Zhang, Z. Y.; Wolfbeis, O. S. *Phys. Chem. Chem. Phys.* **2014,** 16, 20009-20012.
21. Som, S.; Das, S.; Yang, C. Y.; Lu, C. H. *Opt. Lett.* **2016,** 41, 464-467.
22. Liang, Z.-Q.; Zhao, S.-L.; Cui, Y.; Tian, L.-J.; Zhang, J.-J.; Xu, Z. *Chinese Physics B* **2015,** 24, 037801.
23. Svoboda, K.; Block, S. M. *Annu. Rev. Biophys. Biomol. Struct.* **1994,** 23, 247-285.
24. Qiao, Y.; Di, Z.; Ma, Y.; Ma, P.; Xia, S. *Chin. J. Chem. Eng.* **2010,** 18, 446-454.
25. Haro, P.; del Rosal, B.; Martinez Maestro, L.; Naccache, R.; Capobianco, J. A.; Dholakia, K.; Sole, J. G.; Martin Rodriguez, E.; Jaque Garcia, D. *Nanoscale* **2013**.
26. Andres-Arroyo, A.; Gupta, B.; Wang, F.; Gooding, J. J.; Reece, P. J. *Nano Lett.* **2016,** 16, 1903-1910.
27. Jauffred, L.; Oddershede, L. B. *Nano Lett.* **2010,** 10, 1927-1930.
28. Bhattacharjee, S. *J. Controlled Release* **2016,** 235, 337-351.
29. Kokot, G.; Bespalova, M. I.; Krishnan, M. *The Journal of Chemical Physics* **2016,** 145, 194701.
30. Pesce, G.; Lisbino, V.; Rusciano, G.; Sasso, A. *Electrophoresis* **2013,** 34, 3141-3149.

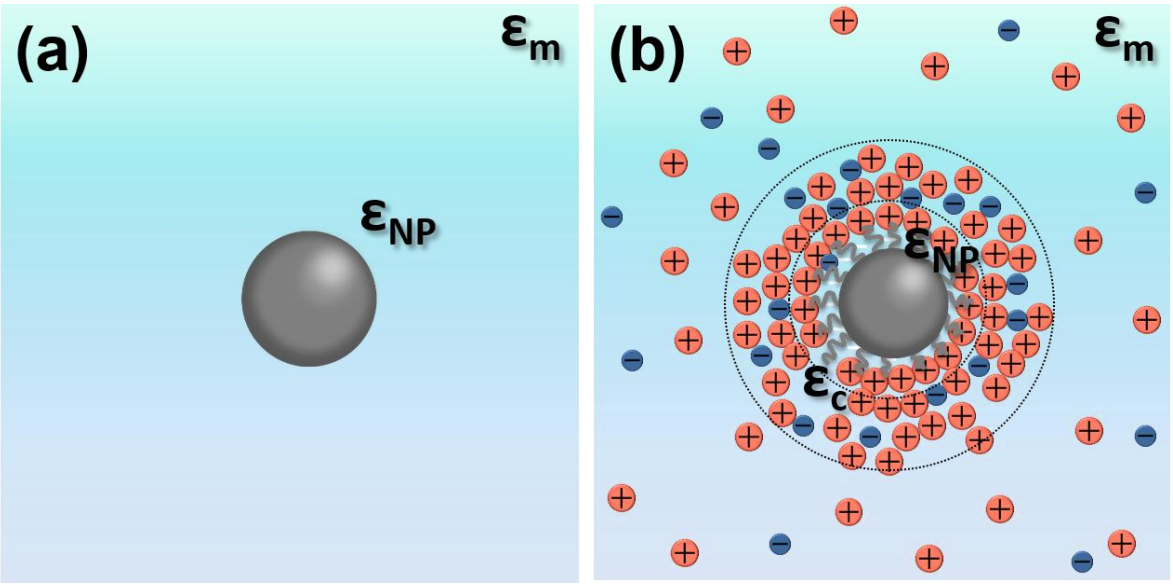

Figure 1. For **(a)** ligand-free NP, the optical force theoretical calculation involves the permittivities of medium (ε_m) and particle (ε_{NP}), while **(b)** in the case of NPs covered with ligands, both particle and coating (ε_C) permittivities are taken into account for optical forces calculations.

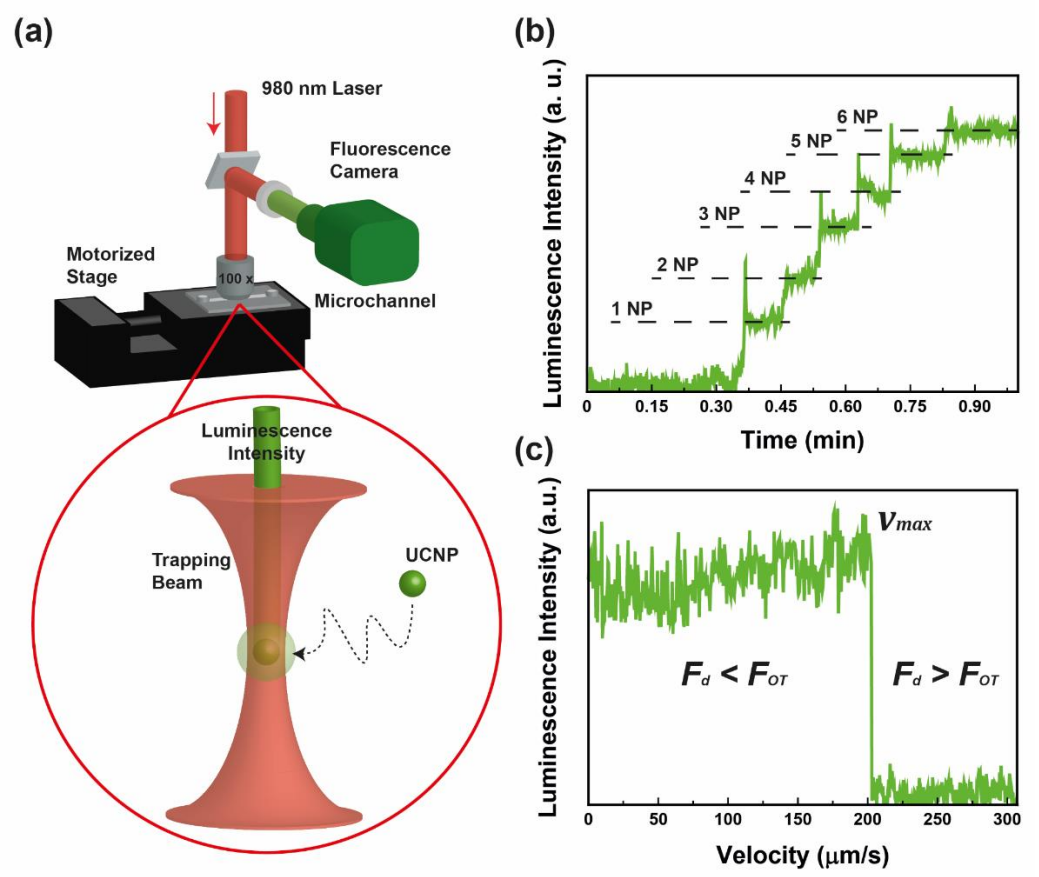

Figure 2. **(a)** Upper part: Experimental setup used for force measurements. Lower part: schematic representation of an optically trapped UCNP. **(b)** Luminescence intensity as a function of time. Each rise represents an UCNP entering the trap. **(c)** Schematic representation of the experimental procedure used for force measurements.

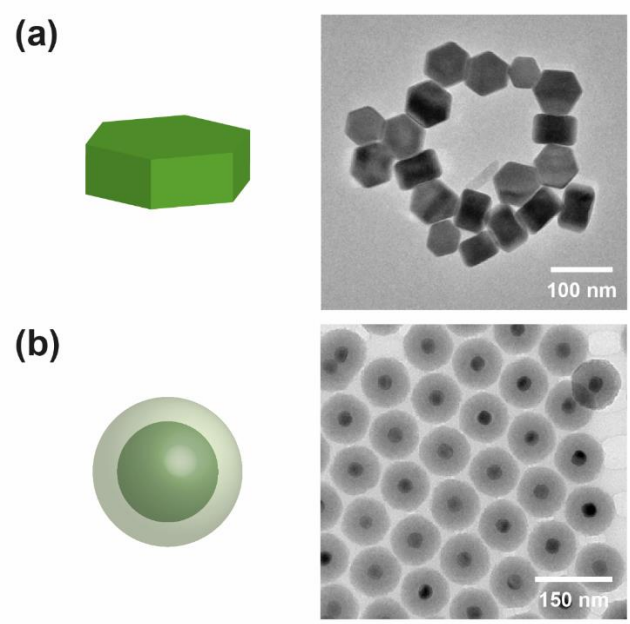

Figure 3. Representative transmission electronic microscopy (TEM) image for the **(a)** disc-like and **(b)** core-shell spherical UCNPs.

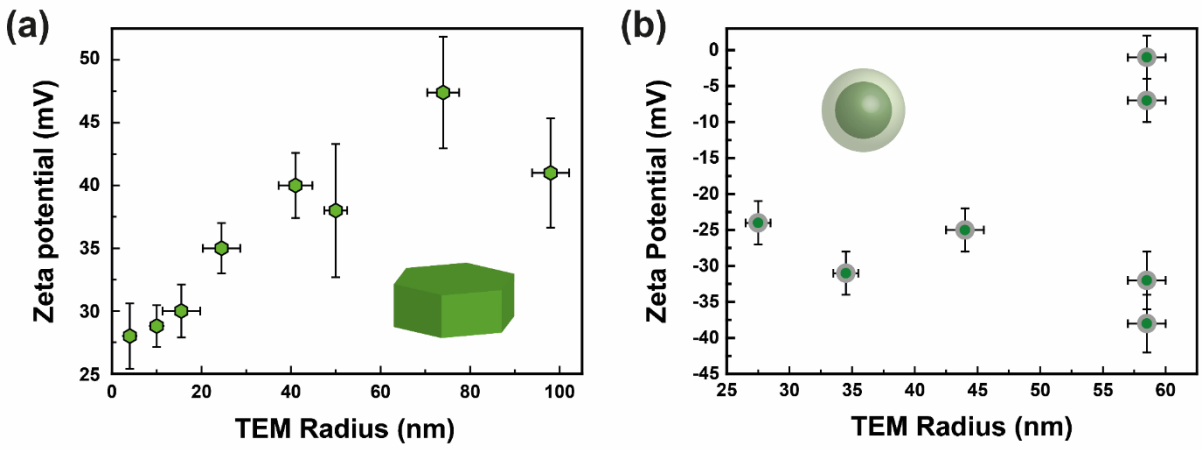

Figure 4. Zeta potential values as a function of the TEM radius for **(a)** disc-like UCNPs and **(b)** core-shell spherical UCNPs.

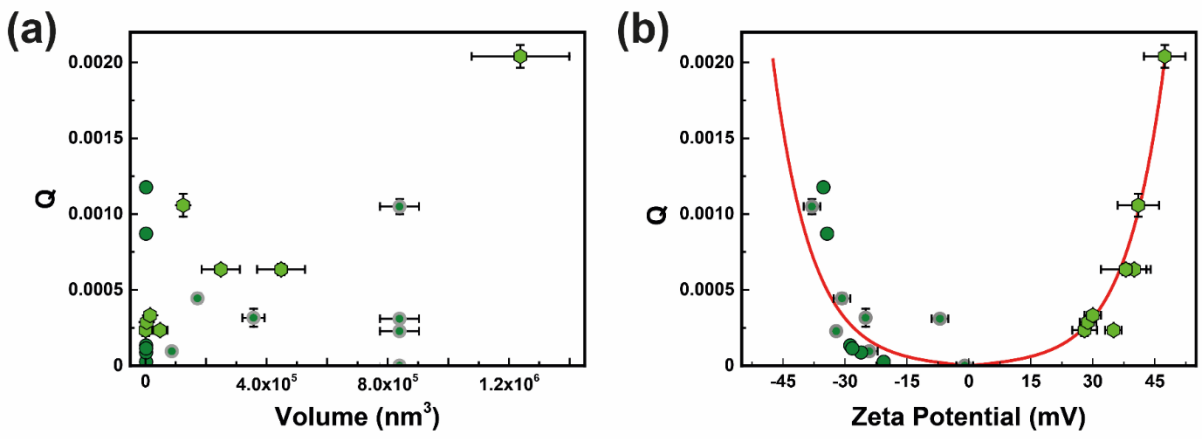

Figure 5. **(a)** Measured Q-factor as a function of the particle volume. **(b)** Q-factor as a function of the zeta potential. Red line is the best fit to equation 10. In both (a) and (b) hexagonal light green dots represent values for disc-like UCNPs, circular grey and green dots correspond to core-shell UCNPs values, and simple dark green dots are values obtained from [17] for 8 nm in diameter UCNPs.

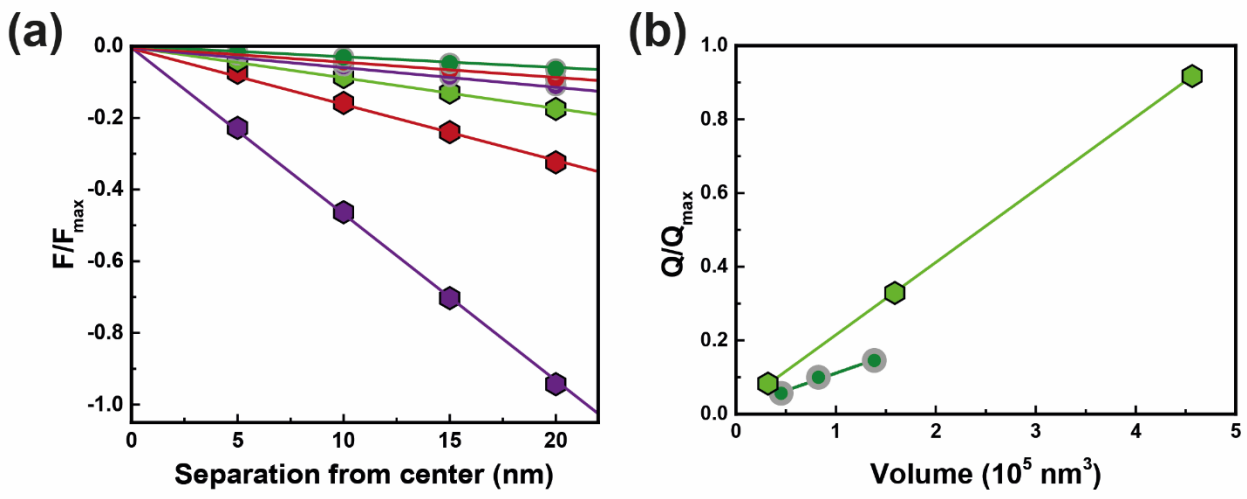

Figure 6. (a) Numerical simulations performed over $NaYF_4$ hexagonal nanoparticles and $NaYF_4$@Sillica core-shell nanoparticles to determine the theoretically predicted evolution of the optical forces as a function of the volume of the particle**. (b)** Dependence of Q-factor on particle´s volume as obtained from calculated data included in (a). Results obtained for hexagonal and core-shell nanoparticles are included. Symbols are calculated data and dashed lines are the best linear fits.

TABLE OF CONTENTS GRAPHIC